Physical limits on the performance of active noise control through open windows

Bhan Lam[1]

Digital Signal Processing Lab, School of Electrical and Electronic Engineering, Nanyang Technological University, Singapore 639798, Singapore

Stephen Elliott

Institute of Sound and Vibration Research, University of Southampton, Highfield Campus, Southampton SO17 1BJ, United Kingdom

Jordan Cheer

Institute of Sound and Vibration Research, University of Southampton, Highfield Campus, Southampton SO17 1BJ, United Kingdom

Woon-Seng Gan

Digital Signal Processing Lab, School of Electrical and Electronic Engineering, Nanyang Technological University, Singapore 639798, Singapore

[1] Electronic mail: blam002@e.ntu.edu.sg

Abstract

Active noise control through open windows is a noise mitigation technique that preserves natural ventilation in dwellings. Designing a practical open window active noise control system requires the knowledge of the physical limits on the attenuation performance. Of the numerous variables to be optimised, it is the control source configuration (quantity and position) that ultimately defines the maximum attenuation attainable by an active noise control system. The physical limits are characterised here by systematically investigating the performance of different physical arrangements of control sources, using a two-dimension simulation model based on the finite-element method, which includes the diffraction effects of the window. The simulations reveal that the best attenuation is achieved by placing the control sources away from the edges of the window. It also shows that the plane of control sources can be placed centrally with respect to the depth of the walls, for practical implementation with minimal performance degradation. The simulated attenuation as a function of frequency and window width, for different angles of noise incidence, can be used to provide an estimate of the number of control sources, based on the desired level of attenuation. This estimate helps to determine the configuration with the minimum number of control sources required for different scenarios, before a more detailed system design is undertaken.

Keywords: Active Noise Control, Finite Element Method, Open Window

1. INTRODUCTION

Common noise mitigation measures such as double-glazed windows and the installation of noise barriers have been somewhat effective, however, these techniques do not translate well for densely populated high-rise urban areas. As barriers only mitigate noise in the shadow zone, upper floors of a high-rise building are typically not shielded from noise [1]. Although integration of active noise control technology on the top of the noise barriers can increase the effective height of the barriers [2,3], land scarcity, cost, and visual aesthetics are several factors that restrict noise barrier implementation. For regions with hot and humid weather, natural ventilation is a priority, as this requirement is usually mandated by local Governments. Thus, in these areas, noise mitigation measures must be effective in a high-rise scenario whilst also maintaining adequate natural ventilation.

Modified ventilation windows have been developed based on the benefits of double-glazing to achieve acoustical shielding while providing some degree of air flow into buildings. The plenum window design proposed by Tong and Tang [4,5], achieved up to 9.5 dBA of noise reduction in a full-scale study. Active noise control systems have also been integrated with 'double-glazed' ventilation systems to achieve better low frequency attenuation [6,7]. Whilst modified ventilation windows can provide significant noise insulation, the air flow rate can be reduced by up to 2 – 4 times [6]. Installation of such ventilation windows also requires existing windows and their supporting structures to be replaced, increasing the cost of implementation and inconvenience to residents.

To retain the full natural ventilation properties of conventional windows, active control methods have emerged as potential solutions. Emms and Fox demonstrated the feasibility of sound attenuation through a square aperture based on the active sound absorption method, an application of the Huygens principle [8,9]. Realization of active sound absorption, however,

requires a continuous distribution of monopole and dipole sources that are susceptible to instability due to uncertainties in calibration [9]. Active noise control (ANC) methods – increasingly found in consumer headphones – can potentially reduce noise in the entire room by controlling the total sound power transmitted through the windows [1]. Although ANC systems for window applications require numerous transducers, sensors and digital processors, the advent of cheaper and more advanced electronics have increased its cost-effectiveness. Scale-model ANC systems (built on open apertures) can achieve wide-band noise reduction of up to 10 dB [10,11], which is similar to modified ventilation windows. ANC systems have also been employed to reduce noise through a partially-opened window [12–14].

The effectiveness of ANC systems is evaluated by how well the 'anti-noise' field minimises the noise in the desired area (e.g., a room). Total or global minimisation of noise in a room can be achieved by (1) controlling all unwanted acoustic modes in the room, or (2) by minimising the acoustic power of the noise source [15,16]. Controlling room modes is considered the least practical solution, as large numbers of control sources would have to be installed in the room. If the source of noise is assumed to be transmitted into a building primarily through the windows, global noise attenuation can be attained if the active noise control system succeeds in controlling the total acoustic power transmitted through the windows.

Noise incident at the façade of the building can be assumed to be plane waves, as surface transportation noise (e.g., busy highway) is usually modelled as an incoherent line source in the far-field [17]. Plane waves through a rectangular aperture exhibit frequency-dependant scattering patterns [9,18,19], and thus the open window ANC systems must also control scattering to achieve global attenuation. However, theoretical studies of the open window ANC systems have only been conducted in free-field conditions [10] and have not considered the physical effects due to the scattering behaviour of the window. Moreover, placement of secondary sources in experiments have been motivated by Huygens principle in the free-field

[10] and by boundary control [11], without taking into consideration the effects of scattering by the window.

The effects of scattering on the attenuation performance of the open window ANC system are investigated here using numerical methods. Control source positions are investigated for various incidence angles and frequencies to establish guidelines for optimal noise attenuation in the frequency domain. The study is performed using the 2D finite element method (FEM), with a maximum element size of one-sixth of the wavelength at 4 kHz. The 2D model has about 1 million elements and is reasonably quick to run for a variety of geometrical conditions, whereas the corresponding 3D model would need about 120 million elements and it would be too time consuming to run all the cases required to provide physical insight and practical guidelines, of the maximum separation between sources for example, which is the purpose of this study. These guidelines can aid in the design of large scale ANC platforms for the active control of noise through open windows for a range of frequencies and incidence angles. The motivation for this initial study is to investigate the control limit set by the position and the number of secondary sources, for a given set of error sensors, which is in line with the hierarchical method of practical active control system design [20] to determine the fundamental physical limitation of the ANC system [21].

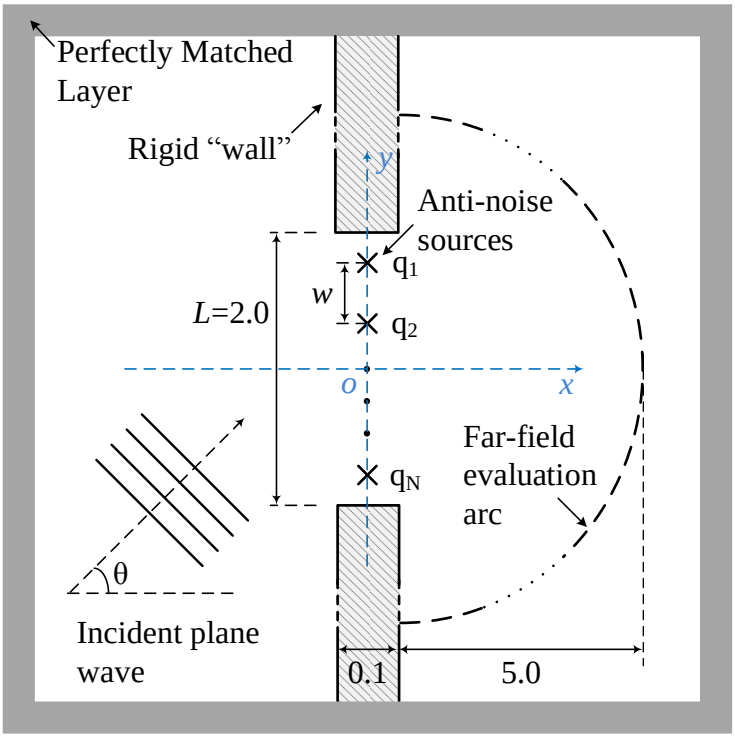

104

105 **Figure 1. 2D FEM model of the active acoustic window (in m). The axes and origin of the**
106 **computation plane is depicted in blue.**

107

108 ## 2. ACTIVE NOISE CONTROL FORMULATION

109 ### 2.1 Design of the active acoustic window model

110 The 2D FEM computation model illustrated in Figure 1 is a 10 m by 10 m free-field cross-
111 section containing a solid wall with a $L = 2$ m wide aperture, bounded by a perfectly-matched
112 layer to emulate a free-field condition. Two rectangular blocks with rigid boundary conditions
113 represent the walls and form the cross-section of the opened window, indicated by the shaded
114 regions in Figure 1. The thickness of the wall is set to 0.1 m, since it was found that changing
115 the wall thickness from 0.05 m to 0.3 m had a minimal effect on the sum of squared pressures
116 in the far-field for frequencies of interest (≤ 4 kHz). N secondary sources, arranged

symmetrically w m apart in the L m wide aperture, are optimised to reduce the sum of squared pressures evaluated at the semi-circular boundary in the far-field. The N secondary sources are modelled as line sources producing cylindrical waves as defined in the FEM software used [22].

Owing to complexities of the large computational model, the FEM simulations were performed on a high-performance workstation with a XEON E5-2699 processor (18 cores, 2.3 GHz) and 128 GB of memory. The density of the mesh was set to provide a minimum of six elements per wavelength at 4 kHz for all frequencies tested (≤ 4 kHz) to ensure consistency and accuracy, giving a 2D mesh consisting of approximately 1 million elements and solved for 2 million degrees of freedom.

2.2 Global control formulation

The active acoustic window concept achieves global attenuation in the building interior by treating the open window as the noise source and minimising its total power output [11,23]. The active noise control system is thus formulated to minimise the sum of squared pressures on the far-field semi-circular array that encompasses the entire open window and all secondary sources. Since the focus of this study is to understand the effects of diffraction on the performance of the active control system, the area to be controlled is assumed to be a free-field.

In the simulations presented here, the acoustic pressures were measured at 1100 positions at a distance of 5 m from the centre of the window as shown in Figure 1, so that the separation between the measurement points was less than one-sixth of a wavelength at the highest frequency of interest.

The vector of complex pressures at all the evaluation positions on the far-field arc can be expressed as

$$\mathbf{e} = \mathbf{d} + \mathbf{G}\mathbf{q}_s, \tag{1}$$

where $\mathbf{d}$ is the vector of complex pressures at the evaluation positions due to the scattered incident plane waves through the window, $\mathbf{q}_s$ is the vector of source strengths of all the secondary sources, and $\mathbf{G}$ is the matrix of complex plant responses between the secondary sources and the evaluation positions on the far-field arc. Both $\mathbf{d}$ and $\mathbf{G}$ were obtained through the FEM simulation. The sum of squared pressures at the evaluation positions is minimised using the exact least squares method with the cost function given by

$$J = \mathbf{e}^{\mathrm{H}}\mathbf{e} = \mathbf{q}_s^{\mathrm{H}}\mathbf{A}\mathbf{q}_s + \mathbf{q}_s^{\mathrm{H}}\mathbf{b} + \mathbf{b}^{\mathrm{H}}\mathbf{q}_s + \mathbf{d}^{\mathrm{H}}\mathbf{d}, \tag{2}$$

where $\mathbf{A} = \mathbf{G}^{\mathrm{H}}\mathbf{G}$ and $\mathbf{b} = \mathbf{G}^{\mathrm{H}}\mathbf{d}$.

By setting the derivative of the cost function in (2) with respect to the real and imaginary components of $\mathbf{q}_s$ to zero [21], a set of optimised secondary source strengths is obtained, given by

$$\mathbf{q}_s = -(\mathbf{G}^{\mathrm{H}}\mathbf{G} + \beta\mathbf{I})^{-1}\mathbf{G}^{\mathrm{H}}\mathbf{d}, \tag{3}$$

where β is a parameter that regularises the matrix to compensate for the ill-conditioning that arises from the overdetermined problem [21], $\mathbf{I}$ is an identity matrix, and $^{\mathrm{H}}$ is the Hermitian operator. The regularisation parameter was set to the minimum value necessary to obtain a well-conditioned inverse of the matrix in brackets in Eq. (3).

2.3 Evaluation parameters

The acoustic power radiated through the window from the primary noise source can be determined by the sum of squared pressures evaluated in the far-field on an enclosing surface [15], which can be written as

$$W_d = \frac{|\mathbf{d}|^2}{2\rho_0 c_0}\pi r, \tag{4}$$

where ρ_0 is the density of air, c_0 is the speed of sound in air, and r is the radius of the evaluation arc. The acoustic power after ANC is calculated similarly, based on contributions from both the noise and secondary sources as

$$W_e = \frac{|\mathbf{e}|^2}{2\rho_0 c_0}\pi r. \tag{5}$$

The attenuation performance of the active acoustic window system is then defined as (5), normalised by (4), and this can written as

$$Attenuation = -10\log_{10}\frac{W_e}{W_d}. \tag{6}$$

Figure 2 shows the sound pressure distribution of example simulations at 100 Hz and 500 Hz before control (left column), and after activating ANC using a single secondary source at the centre of the window, optimised to reduce the acoustic power transmitted through the window opening. The transmitted field is clearly reduced more at 100 Hz than it is at 500 Hz, to an extent that will be quantified in the following section.

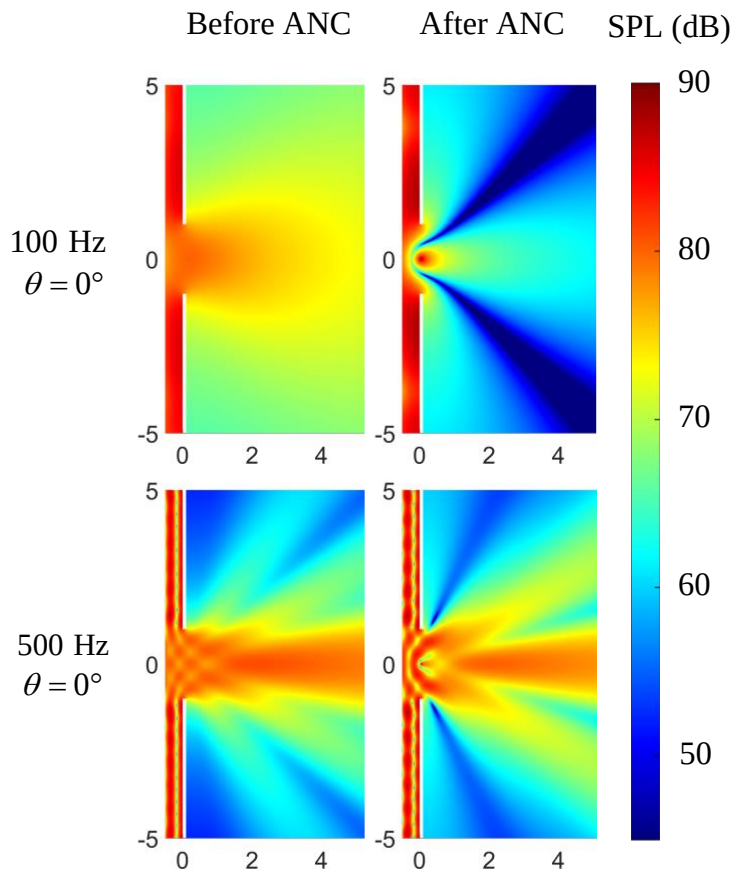

Figure 2. Sound pressure distribution using one secondary source centred at (0, 0) to control the sound power for single tone (100 and 500 Hz) with noise incidence angle at $\theta = 0°$.

3. SECONDARY SOURCE POSITIONING

Based on Huygens principle, Murao and Nishimura [10] identified that the separation distance between the secondary sources was as an important factor affecting the attenuation performance of the active acoustic window system in the free-field. When the effects of scattering around the edges of the window are considered, however, the design of the ANC system based on this separation distance alone is insufficient. Additional factors that can potentially affect the performance of the ANC system include, placement of the secondary sources relative to the depth of the wall, and the proximity of the sources to the edges of the

window. Due to the lack of an established analytical solution to the window problem, (1) the effect of source separation (*y*-axis) and hence, the number of sources required, and (2) the source placement relative to the depth of the wall (*x*-axis), are systematically evaluated using the finite element models.

3.1 Secondary source separation

The separation distance between secondary sources, w, indirectly dictates the number of sources required in a finite aperture. More importantly, w also determines the cut-off frequency at which the ANC system will fail, as determined in a free-field study with an infinite array of sources [24,25]. Although it is intuitive that sources should be evenly distributed across the aperture for normal incidence plane wave, the separation distance between the sources w can span from $L/(N+1)$ to $L/(N-1)$ m, depending on how close the peripheral sources of the array are to the edge of the wall.

The effect of source separation, w, on the attenuation performance is explored for increasing number of sources N. Only frequencies up to 4 kHz are considered, which corresponds to the upper limit of the traffic noise spectrum in conjunction with the upper limit of practical ANC performance. In the FEM simulations, the plane wave noise source is incident at $\theta = 0°$, and secondary sources are fixed at $x = 0$ m. The sources are distributed symmetrically about the x-axis and separated by a distance of w m, as exemplified in Figure 3(a) and (b) for $N = 2$ and $N = 3$ respectively.

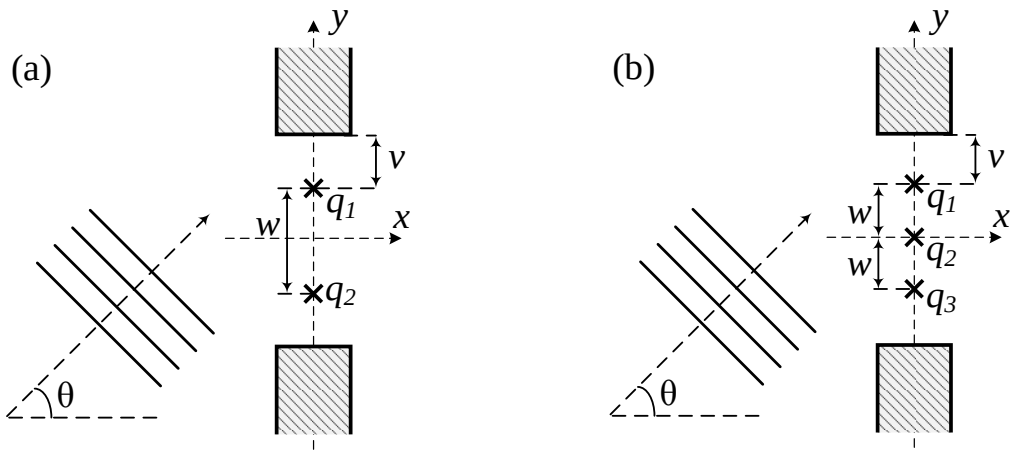

Figure 3. Secondary sources symmetrically positioned about the x-axis, at $x = 0$ m, and with separation distance for (a) $N = 2$ sources with $0.01 \leq w < 2$ m, and (b) $N = 3$ sources with $0.01 \leq w < 1$ m.

To provide a clearer representation of the results, the gap from the wall edge to the nearest source is considered, labelled as v in Figure 3 and defined to be

$$v = \frac{L - w(N-1)}{2}. \tag{7}$$

Hence, v equals zero if $w = L/(N-1)$, and v approaches w as w approaches $L/(N+1)$ m.

The general trend observed across all cases of N in Figure 4 shows that the attenuation performance degrades sharply as v approaches w, when $\pi < kw < 2\pi$, where k is the acoustic wavenumber, which is equal to 2π divided by the wavelength. As N increases, the attenuation performance peaks at $v = w/2$ regardless of kw, as seen in Figure 4 (b) to (d), for frequency range $\pi < kw < 2\pi$. Hence, it is evident that sources should not be positioned at the edge even for large N (small w), as may have been expected from the literature on the active control of sound diffracted over barriers [3,26]. Based on an evaluation of the results for $N \geq 5$, a uniform and symmetric distribution of sources is suggested, where $v = w/2$ and so w is given by

$$w = \frac{L}{N}. \tag{8}$$

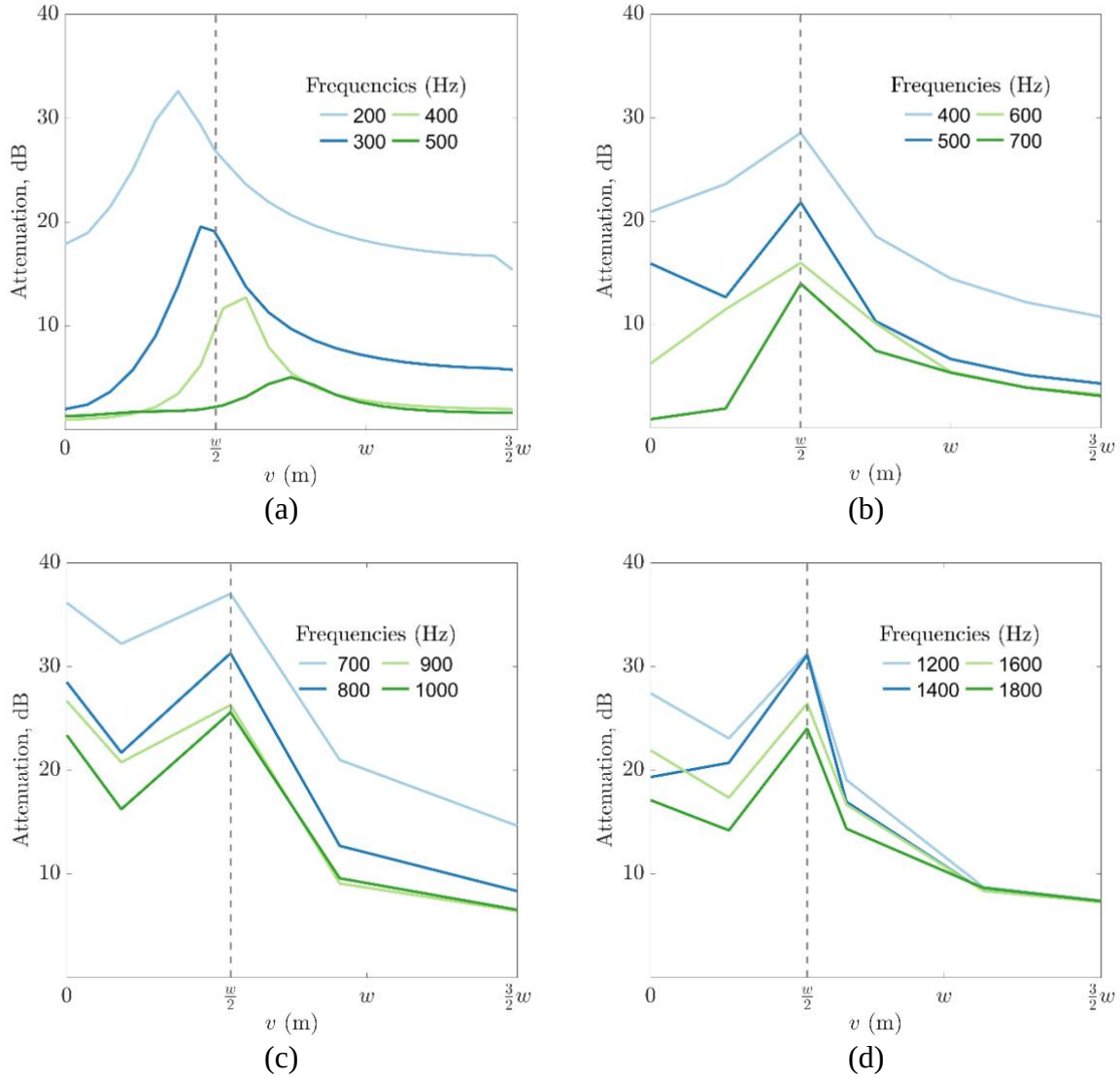

Figure 4. Attenuation performance as a function of separation distance w represented by changes in the gap v, when (a) $N = 3$, (b) $N = 5$, (c) $N = 9$, and (d) $N = 13$ sources. The dashed line indicates when $v = w/2$ m.

3.2 Location of secondary sources along the depth of the aperture

The effect of scattering is prominent when the wavelength of the primary source is large compared to the size of the aperture ($\lambda > L$) [9,24,25], as depicted in the 100 Hz example before control in Figure 2. To understand the degree of significance of the secondary source positions along the depth of the aperture, i.e., along the x -axis in Figure 1, on the attenuation performance, simulations were conducted with $N = 5,\ 7,\ 9,$ and 13 sources. The separation distance w is selected using the guideline in Eq. (8) so that $w = 0.4$ m, 0.286 m, and so forth, for corresponding values of N .

The results for $N = 5$ are shown in Figure 5(a), from which it can be seen that the x -axis position has no significant effect on the performance of the ANC system for frequencies at which the attenuation is at least 10 dB.

The results for $N = 13$ is shown in Figure 5(b), in which the control performance degrades rapidly when secondary source positions are situated beyond $x = 0.02$ m, for the frequencies plotted. Control performance at lower frequencies (i.e., $kw < \pi$) are rather constant with x locations farther from the control zone ($x < 0$ m), but start to degrade by as much 30 dB when $x > 0$ m. This observation suggests that the array of secondary sources struggle to generate anti-noise waves that can match and attenuate the scattered primary noise waves, as the array is situated farther away from the primary source (aperture).

For frequencies in the range of $\pi < kw < 2\pi$, however, control performance degrades as the sources are situated both farther into ($x > 0$ m), and away ($x < 0$ m) from the control zone. Maximum control is attained when secondary sources are located along x positions between 0 and 0.02 m. At frequencies approaching the spatial aliasing limit, the resolution of the reconstructed anti-noise plane waves becomes increasingly poor.

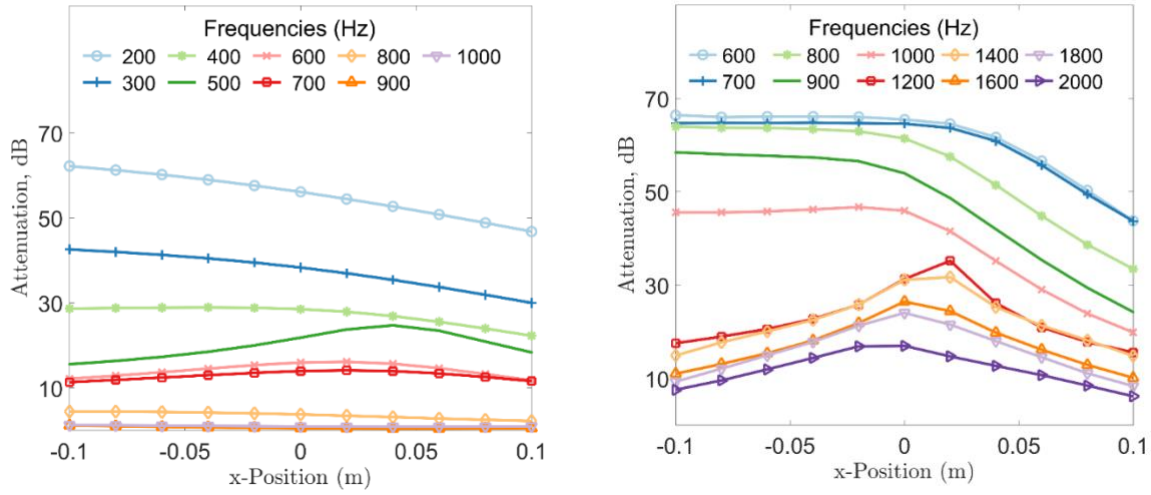

(a) (b)

Figure 6. Attenuation performance of (a) $N = 5$**, and (b)** $N = 13$ **sources, uniformly distributed between** y **= -0.8 and 0.8 m at intervals of** $w = 0.4$ m, **and between** y **= -0.9231 and 0.9231 m at intervals of** $w = 0.1538$ m, **respectively.** x **positions vary from** $-0.1 < x < 0.1$ m**, and with plane primary wave incident at** $\theta = 0°$, **for different frequencies.**

Overall, placing the plane of the secondary sources at $x = 0$ m, i.e., in the centre of wall with respect to its depth, gave the best average performance, so this position was used in the further simulations.

The central location of the control source array yielding the best average performance coincides with the distribution of normal velocities within the depth of the wall. At low frequencies, the primary normal velocity distribution is similar along the depth of the wall, as reflected in Figure 5 for x-axis positions at $x = -0.05$ m (green dotted line), $x = 0$ m (solid pink line), and $x = 0.05$ m (yellow line with solid circle markers). The low variability in the primary normal velocity distributions along the wall depth coincides with the consistent attenuation performance at x-axis positions along the wall depth at low frequencies. As the frequency increases, the magnitude of the primary normal velocities appears to fluctuate the least intensely at $x = 0$,

again coinciding with the best average attenuation performance when the control source array is placed at $x = 0$.

4. PERFORMANCE AS A FUNCTION OF FREQUENCY AND ANGLE OF INCIDENCE

For a finite aperture, the minimum number of sources required is based on the frequency upper bound and dominant angle of incidence for global control. Firstly, the upper frequency limit of control for different source configurations is determined for impinging plane waves at normal incidence. Secondly, the maximum separation distance for good control and its respective cut-off frequency is generalised as a function of normalised frequencies for different source configurations, also for normal incident plane waves. Lastly, the generalisation is extended to include oblique incidence angles.

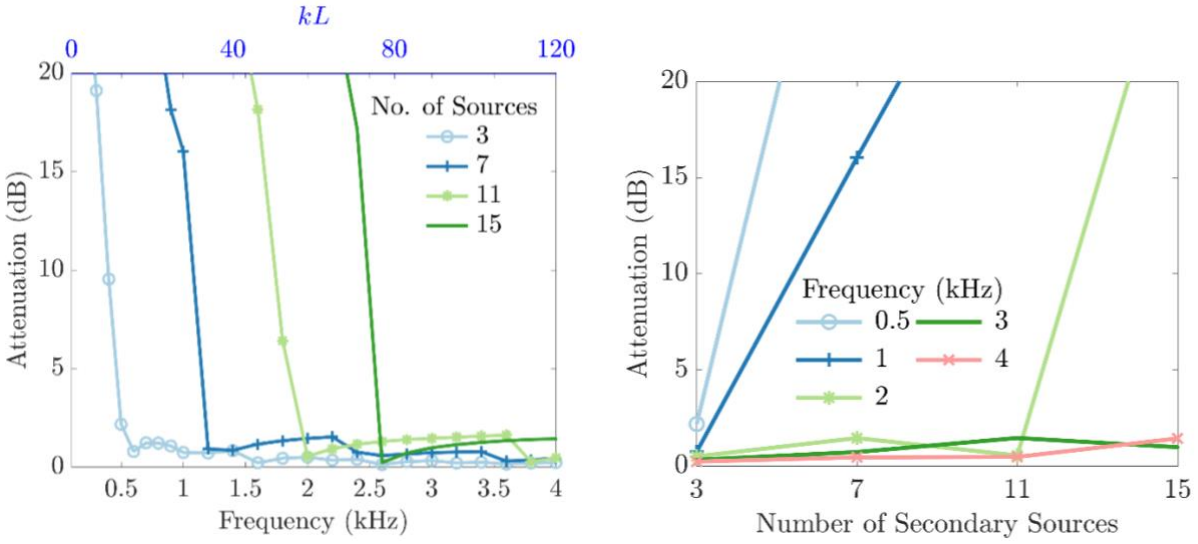

(a) (b)

Figure 7. Attenuation performance using different number of sources, (a) as a function of frequency, and (b) as a function of number of secondary sources, for a noise incidence of $\theta = 0°$, and all sources located at $x = 0$ m.

4.1 As a function of frequency at normal incidence

A cut-off frequency, above which the performance is poor, is clearly illustrated in Figure 6(a) for cases when N is equals to 3, 5, 7, 11 and 15 sources, which is consistent with that identified in [24,25], for the 2D and 3D free field case. By plotting the attenuation as a function of N for selected frequencies, the minimum number of sources required for good global control (>20 dB) can be deduced, as shown in Figure 6(b). For instance, at least 9 sources are required to obtain good global control up to 1 kHz, for this aperture of width $L = 2$ m.

Figure 7 shows the sound pressure level (SPL) distribution plots of selected frequencies for different number of secondary sources, N. In cases where good control is achieved, such as when $N = 7$ at 500 Hz, complex residual sidelobes are present in the near field. This suggests that in practical applications of active control, the error microphones should be placed at a sufficient distance away. Based on the free-field analytical analysis of an infinite plane array of sources, the error microphones should be placed at least half the separation distance away for frequencies at which w is less than half a wavelength [25]. From observation of other instances of good control in Figure 7 and as suggested by Elliott et al. [25], the error microphones should be greater than half the source separation distance away at higher frequencies due to more complex and intense near-field sound pressures.

In cases beyond the cut-off frequencies in Figure 6(a), such as at 2 kHz with $N = 7$, there is an undesired increase of sound pressure at other areas outside the noise main lobes, as depicted in the corresponding plots of Figure 7. Hence the frequency range of the controller should be limited to avoid such high-frequency enhancements.

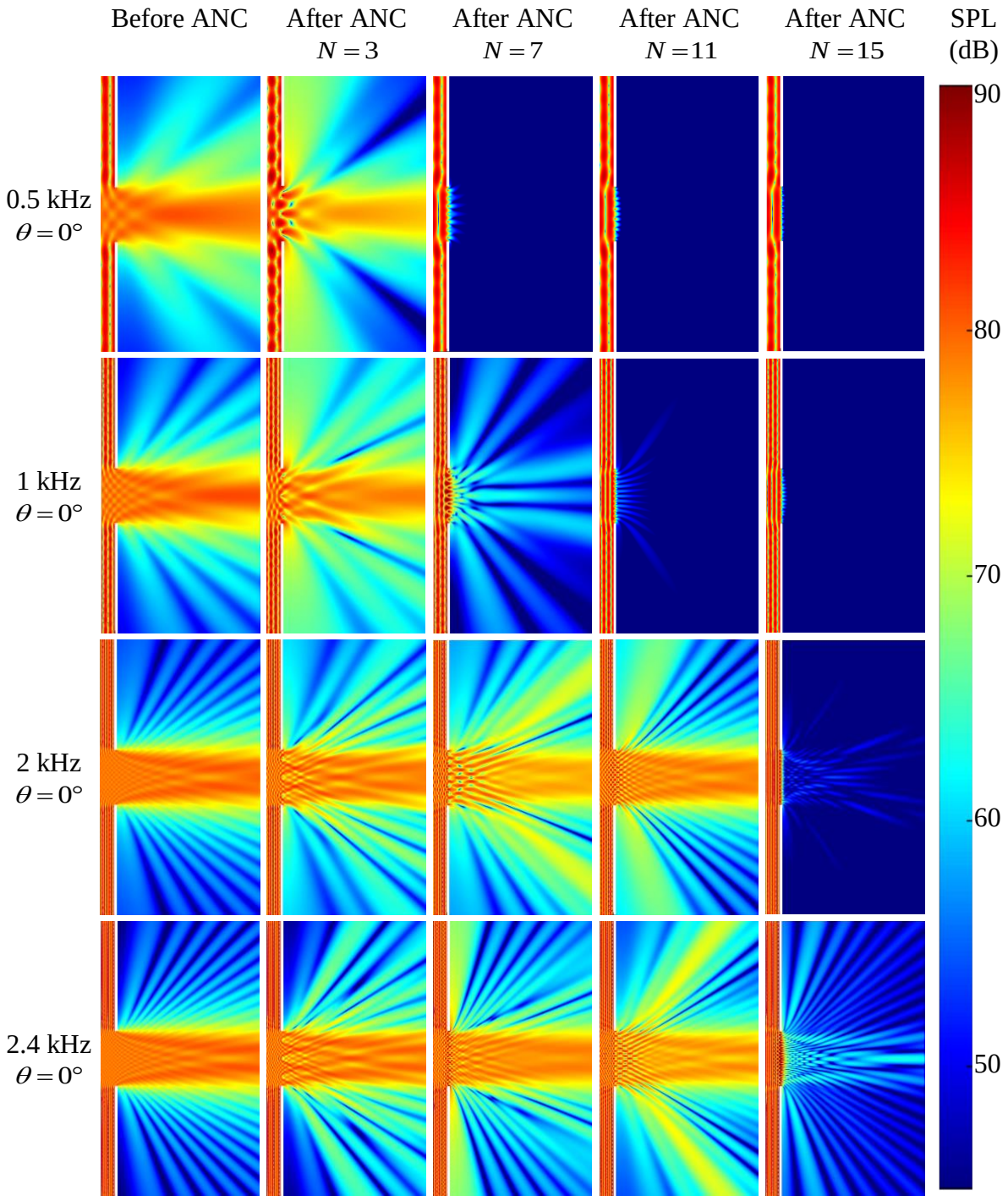

Figure 8. Sound pressure level distribution plots for two frequencies at $\theta=0°$ and $x=0\,\mathrm{m}$ for $N=3$, $N=7$, $N=11$, and $N=15$.

291

292

4.2 Maximum separation distance

To determine the maximum separation distance, and hence the total number of sources required to achieve global reduction for an aperture of variable size, the attenuation performance is plotted as a function of kw. The results for six different separation distances, w, are shown in Figure 8, namely, with N equals to 2, 3, 5, 7, 9, and 13, and w set using Eq. (8). The array of sources is situated at $x = 0$ m, and a primary plane wave impinging at $\theta = 0°$ incidence. The results of $N = 1$ is included in Figure 8, for reference, with w set to 1.

When $kw < \pi$, the attenuation performance was at least 20 dB for $N > 2$ sources, where the separation distance w is less than half the acoustic wavelength. Attenuation performance terminates at frequencies $kw \geq 2\pi$, in line with the free-field cases [24,25] and as shown evidently in Figure 8. It is also worth noting that as N increases, the minimum separation distance approaches λ instead of $\lambda / 2$. While using this guideline, one must keep in mind that these results are the theoretical limits of the ANC system and must consider the lost in fidelity when electronic systems are implemented.

As the acoustic window is required to attenuate noise from different dominant incidence angles (e.g., control of traffic noise at the upper floors of high-rise buildings), the active control performance is investigated in the following sub-section for different noise source incidence angles.

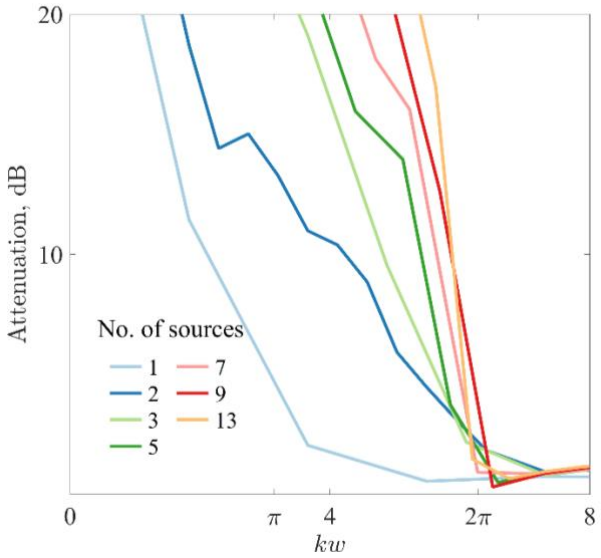

Figure 9. Attenuation performance using different number of sources, as a function of frequency and separation distance, at noise incidence $\theta = 0°$, and all sources are located at $x = 0$ m.

4.3 Performance at different angles of incidence

Oblique noise incidences are cases analogous to noise impinging on windows at different levels of a high-rise building. For instance, an incidence angle of $60°$ corresponds to an approximate position at the tenth storey of the building (for a road at surface level, 100 m away from the building).

As the angle of incidence increase, the cut-off frequencies decreases as shown in Figure 9 for incidence angles θ at (a) $30°$, (b) $60°$, and (c) $90°$. The corresponding minimum number of sources to achieve 20 dB of attenuation at 1 kHz increased from $N = 9$, for the normal incidence case

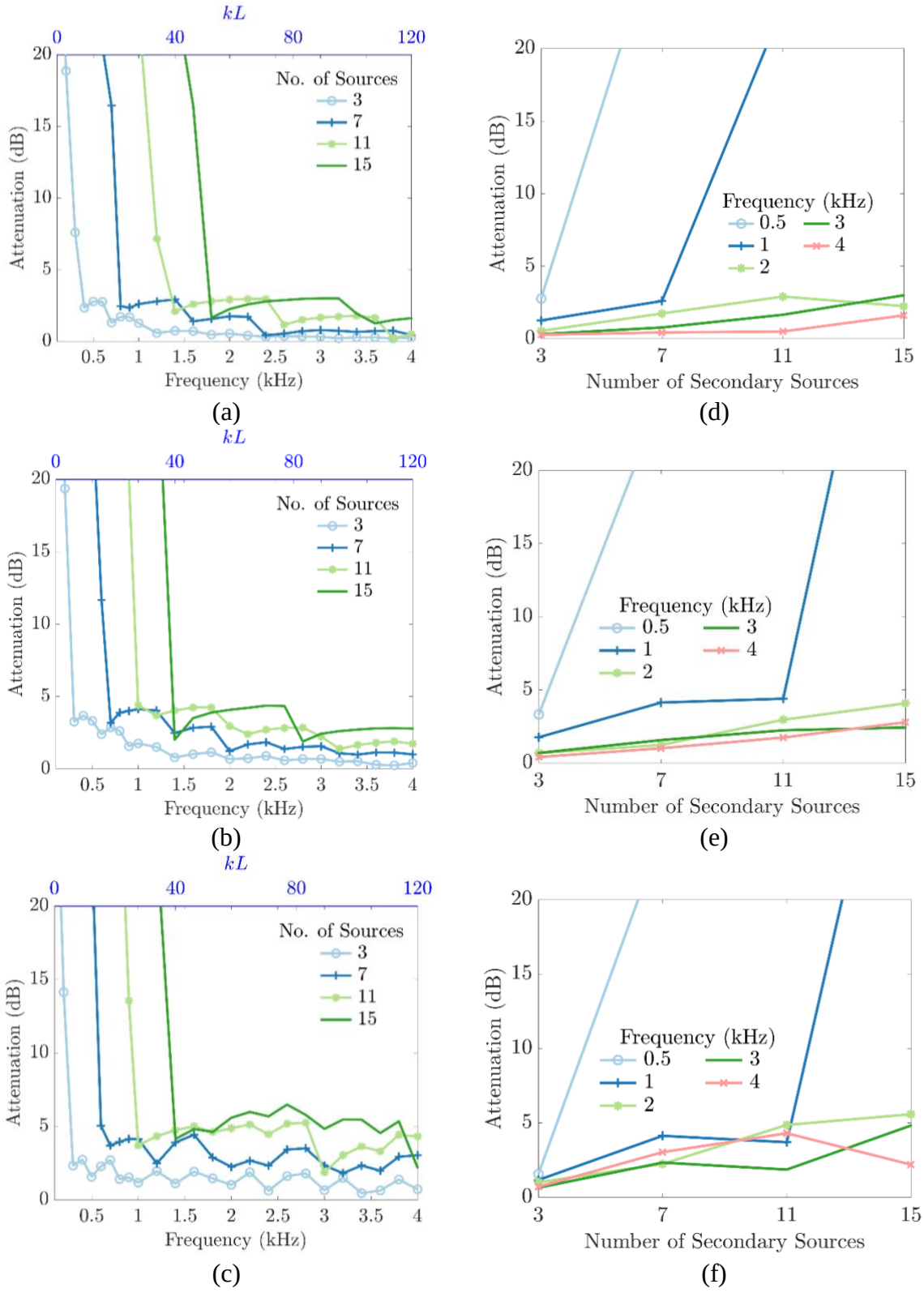

Figure 10. Attenuation performance using different number of sources, as a function of frequency for noise incidence θ at (a) $30°$, (c) $60°$, and (e) $90°$; and as a function of number of secondary sources, of noise incidence θ at (b) $30°$, (d) $60°$, and (f) $90°$.

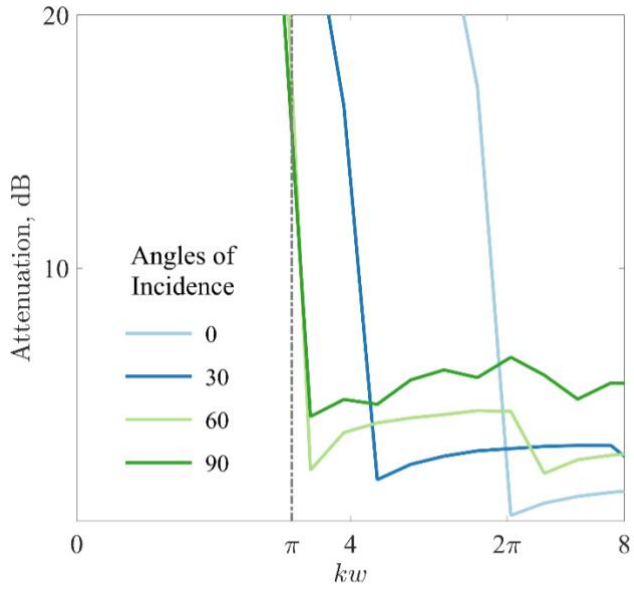

Figure 11. Attenuation performance for $N=15$ and incidence angles up to $\theta=90°$, as a function of kw.

in section 4.1, to $N=11$ for $\theta=30°$, and $N=13$ for $\theta=60°$ and $90°$, as shown in Figure 9 (d), (e), and (f), respectively.

To illustrate the effect of oblique incidences on the minimum source separation distance w for good global control, the attenuation is plotted as a function of kw for different values of θ, when $N=15$, as shown in Figure 10. The cut-off frequencies in Figure 10 show that for frequencies up to $90°$, the separation distance has to be less than half the wavelength ($kw<\pi$). These results are in line with the guideline determined from the free field analysis [24,25], such that $w<\lambda/(1+\sin\theta)$.

The findings can be further generalised by taking the window size, L, into consideration. Since $w=L/N$, N can be decided based on $w<\lambda/(1+\sin\theta)$ to give

$$N>\left\lceil\frac{L(1+\sin\theta)}{\lambda}\right\rceil, \text{ for all } \theta\le 90°,\ N\in\mathbb{Z}^{+} \tag{9}$$

where N is a positive integer $\in \mathbb{Z}^+$, and $\lceil L(1+\sin\theta)/\lambda \rceil$ is the ceiling function that yields the smallest integer $\geq L(1+\sin\theta)/\lambda$. As seen from Figure 9(e) and from Eq. (9), more than 11 sources are needed if $\theta = 60°$ for frequencies up to 1 kHz.

5. CONCLUDING REMARKS

The fundamental physical limits of active noise control (ANC) for open windows is explored here using 2D finite element numerical simulations. The noise source has been assumed to be far away and so generates an incident plane wave, and the active control system has been formulated to control the total noise power entering the window into a free-field environment. The effect of source positioning within the window is considered first. To maximise the controllability, it was found that the sources should not be placed at the edge of the walls within which the window is mounted. It was also observed that the array of secondary sources exhibited good overall performance when situated in the centre of the walls with respect to its depth, increasing the practicality of the ANC system. The detailed acoustics behind these observations probably depend on the nature of the diffracted sound field at the edges of the window, but since the analysis of such effects is known to be rather complicated, this theoretical analysis is left as future work.

It was found that when the noise is normally incident, the sound power transmitted through the window could be attenuated by about 20 dB if the separation distance between the secondary sources, w, was less than a wavelength. When the angle of incidence is greater than 0 degrees up to about 90 degrees, however, as it may well be for upper stories of a high building next to a noisy road, the performance is degraded, so minimum w is less than $\lambda/(1+\sin\theta)$. These findings can be used to estimate the number of secondary sources required in practice to

provide a given level of control at a given frequency for a given angle of incidence. For example, a different number of secondary sources may be required depending on which storey the system is to be installed, as this will influence the dominant angle of incidence.

Although the limits of attenuation performance have been determined in 2D simulations, it seems reasonable to assume that the guidelines on the maximum separation of the sources will also be carried over to the practical, 3D, situation. This assumption stems from the free-field case [24], where deviation in propagating modes between 2D and 3D simulations only occurred at normalised frequencies kw larger than 2π, at which control is poor for all angles of incidence.

Successful translation into a practical ANC system requires further investigation into the cost function to be minimised, the error sensor placement, the quality of the reference signal, and finally the signal processing algorithm [27,28] and hardware used [29].

Experimental validation of the study on a test model with actual windows is currently underway [30]. The present study, of the fundamental physical limitations of such a system, can help to provide estimates of the number of secondary sources required to achieve good performance for a given situation in practice, and thus at least provide an estimate of the minimum number of channels required before the more detailed design work is undertaken.

ACKNOWLEDGEMENT

This material is based on research/work supported by the Singapore Ministry of National Development and National Research Foundation under L2 NIC Award No.: L2NICCFP1-2013-7

References

[1] Lam B, Gan W-S. Active Acoustic Windows: Towards a Quieter Home. IEEE Potentials 2016;35:11–8. doi:10.1109/MPOT.2014.2310776.

[2] Chen W, Rao W, Min H, Qiu X. An active noise barrier with unidirectional secondary sources. Appl Acoust 2011;72:969–74. doi:10.1016/j.apacoust.2011.06.006.

[3] Fan R, Su Z, Cheng L. Modeling, analysis, and validation of an active T-shaped noise barrier. J Acoust Soc Am 2013;134:1990–2003. doi:10.1121/1.4817887.

[4] Tong YG, Tang SK. Plenum window insertion loss in the presence of a line source—A scale model study. J Acoust Soc Am 2013;133:1458–67. doi:10.1121/1.4788996.

[5] Tong YG, Tang SK, Kang J, Fung A, Yeung MKL. Full scale field study of sound transmission across plenum windows. Appl Acoust 2015;89:244–53. doi:10.1016/j.apacoust.2014.10.003.

[6] Huang H, Qiu X, Kang J. Active noise attenuation in ventilation windows. J Acoust Soc Am 2011;130:176–88. doi:10.1121/1.3596457.

[7] Qiu X, Huang H, Lin Z. Progress in research on natural ventilation ANC windows. INTER-NOISE NOISE-CON Congr. Conf. Proc., Institute of Noise Control Engineering; 2011, p. 3189–96.

[8] Emms GW, Fox C. Control of sound transmission through an aperture using active sound absorption techniques : a theoretical investigation. Appl Acoust 2001;62:735–47. doi:10.1016/S0003-682X(00)00063-3.

[9] Emms GW. Active sound power absorbers: their effect on sound transmission thorugh wall openings. PhD Thesis, The University of Auckland, 2000.

[10] Murao T, Nishimura M. Basic Study on Active Acoustic Shielding. J Environ Eng 2012;7:76–91.

[11] Kwon B, Park Y. Interior noise control with an active window system. Appl Acoust 2013;74:647–52. doi:10.1016/j.apacoust.2012.11.005.

[12] Pàmies T, Romeu J, Genescà M, Arcos R. Active control of aircraft fly-over sound transmission through an open window. Appl Acoust 2014;84:116–21. doi:10.1016/j.apacoust.2014.02.018.

[13] Carme C, Schevin O, Clavard J. Active noise control at the openning of a compact acoustic enclosure. INTER-NOISE NOISE-CON Congr. Conf. Proc., Hong Kong SAR, China: 2017, p. 1707–13.

[14] Carme C, Schevin O, Romerowski C, Clavard J. Active opening windows. Proc. 23rd Int. Congr. Sound Vib. ICSV23, Athens, Greece: 2016.

[15] Nelson PA, Elliott SJ. Point source and the active suppression of free field radiation. Act. Control Sound, Academic Press; 1992, p. 231–71.

[16] Hansen C, Snyder S, Qiu X, Brooks L, Moreau D. Active control of free-field sound radiation. Act. Control Noise Vib. Second Ed., CRC Press; 2012, p. 823–982. doi:doi:10.1201/b15923-9.

[17] Arenas JP. Use of Barriers. Handb. Noise Vib. Control, John Wiley & Sons, Inc.; 2007, p. 714–24. doi:10.1002/9780470209707.ch58.

[18] Park HH, Eom HJ. Acoustic scattering from a rectangular aperture in a thick hard screen. J Acoust Soc Am 1997;101:595–8. doi:10.1121/1.417971.

[19] Hongo K, Serizawa H. Diffraction of an acoustic plane wave by a rectangular hole in an

infinitely large rigid screen. J Acoust Soc Am 1999;106:29–35. doi:10.1121/1.427033.

[20] Hansen C, Snyder S, Qiu X, Brooks L, Moreau D. Control system implementation. Act. Control Noise Vib. Second Ed., CRC Press; 2012, p. 1357–83. doi:10.1201/b15923-14.

[21] Elliott SJ. The Physical Basis for Active Control. Signal Process. Act. Control, London: 2001, p. 1–48. doi:10.1016/B978-012237085-4/50003-X.

[22] COMSOL Multiphysics. Acoustics Module User's Guide 2015.

[23] Lam B, Elliott SJ, Cheer J, Gan W-S. The Physical Limits of Active Control of Noise through Open Windows. 12th West. Pacific Acoust. Conf., Singapore: 2015.

[24] Elliott S, Cheer J, Lam B, Shi C, Gan W. Controlling Incident Sound Fields With Source Arrays in Free Space and Through Apertures. In: Gibbs BM, editor. Proc. 24th Int. Congr. Sound Vib., London, UK: 2017, p. 1–7.

[25] Elliott SJ, Cheer J, Lam B, Shi C, Gan W. A wavenumber approach to analysing the active control of plane waves with arrays of secondary sources. J Sound Vib 2018;419:405–19. doi:10.1016/j.jsv.2018.01.028.

[26] Hart CR, Lau S-K. Active noise control with linear control source and sensor arrays for a noise barrier. J Sound Vib 2012;331:15–26. doi:10.1016/j.jsv.2011.08.016.

[27] Murao T, Shi C, Gan W-S, Nishimura M. Mixed-error approach for multi-channel active noise control of open windows. Appl Acoust 2017;127:305–15. doi:10.1016/j.apacoust.2017.06.024.

[28] Lam B, He J, Murao T, Shi C, Gan W-S, Elliott SJ. Feasibility of the full-rank fixed-filter approach in the active control of noise through open windows. INTER-NOISE NOISE-CON Congr. Conf. Proceedings, InterNoise16, Hamburg, Germany: 2016, p.

3548–55.

[29] Fasciani S, He J, Lam B, Murao T, Gan W-S. Comparative study of cone-shaped versus flat-panel speakers for active noise control of multi-tonal signals in open windows. INTER-NOISE NOISE-CON Congr. Conf. Proc., San Francisco, CA, USA: 2015, p. 1109–20.

[30] Lam B, Shi C, Gan W. Active Noise Control Systems for Open Windows : Current Updates and Future Perspectives. Proc. 24th Int. Congr. Sound Vib., London, UK: 2017, p. 1–7.